Improved Signal-to-Noise in PET Activation Studies Using Switched Paradigms

Simon R. Cherry, Roger P. Woods, Niraj K. Doshi, Pranab K. Banerjee and John C. Mazziotta

Imaging Sciences Division, Crump Institute for Biological Imaging, Department of Molecular and Medical Pharmacology; Brain Mapping Division, Department of Neurology, UCLA School of Medicine, Los Angeles, California

PET activation studies employing the autoradiographic technique and ^{15}O-water or ^{15}O-butanol use the difference between images acquired under baseline conditions and during activation to detect focal changes in cerebral blood flow which occur upon stimulus presentation. Typically, the activating task or baseline conditions are maintained throughout the entire imaging period. Simulations of the kinetics of these freely diffusible tracers suggest there may be an advantage to switching between activation and baseline conditions during the course of the study which results in images which maximize the difference signal rather than seeking to quantitate blood flow. We examine the potential of these switched protocols to increase signal-to-noise (S/N) in PET activation studies. **Methods:** We examined S/N in activation studies using both standard and switched paradigms with a simple switched protocol and dynamic three-dimensional PET data from human subjects. With tracer kinetic simulations, we investigated the sensitivity of the S/N gain to factors such as the shape of the input function, the time at which the conditions are switched and the magnitude of the activation. **Results:** In human studies of activation sites in the visual cortex, primary motor and premotor areas, S/N improvements of 20%–30% were detected using the switched paradigms. Simulations show that this gain is virtually independent of activation magnitude and that there is a broad time window of 20 sec for making the switch between conditions. To obtain the highest S/N gain, a rapid bolus injection is required. **Conclusion:** Switched paradigms have the potential to significantly increase S/N in PET activation studies. In human studies, the S/N increase averaged 25% which is equivalent to increasing the number of counts collected by 50%. Switched paradigms can be used to maximize the difference signal in many activation studies, and do not preclude the absolute quantitation of blood flow using the standard autoradiographic technique.

Key Words: PET; activation studies; oxygen-15-water

J Nucl Med 1995; 36:307–314

PET is the most widely used noninvasive imaging technique for investigating functional activity in the human brain (*1*). Recently, PET studies have been augmented by data from functional MRI, although this technique is still in its early phases of validation (*2–4*). Methodology for PET activation studies continues to improve dramatically, fueled by the desire to obtain meaningful results from individual subjects. The two key issues are to increase signal-to-noise (S/N) in PET datasets to improve reliable detection of activation foci, and to reduce the radiation dose to the subject to as low a level as possible. By combining three-dimensional PET data acquisition (*5,6*) with the concept of dose fractionation, it has become possible to double the S/N while simultaneously reducing the patient dose by 40% (*7*). Development and improvement of image registration procedures (*8,9*) and statistical analyses of data (*10,11*) have also been responsible for advancing the field. This paper examines a different approach which exploits the tracer kinetics of freely diffusible tracers to further boost S/N in PET activation studies.

A general goal of PET activation studies using ^{15}O-water or ^{15}O-butanol is to detect focal changes in tracer uptake due to a stimulus related change in regional cerebral blood flow (rCBF). The autoradiographic method (*12–14*) is commonly employed for such studies. With this technique, PET data are integrated over a period of 40 sec after tracer arrival in the brain and the task conditions (either activation or baseline) maintained throughout the study period. The integration time is chosen such that the count density in the PET images is almost linearly related to rCBF. Studies obtained in the baseline state are subtracted from those obtained in the activated state to reveal areas of focal rCBF changes.

The autoradiographic method attempts to quantitate absolute or relative changes in rCBF. Another approach is to try and maximize the S/N in the difference images, without worrying whether the images are linearly proportional to rCBF. This leads to slightly longer integration times (in the 60–90 sec range) for optimal S/N (*15,16*). The longer data acquisition time results in a decrease in noise in the PET images, however, at later times the signal is also diminishing rapidly. This is because both the uptake and subsequent washout rates for a freely diffusible tracer such as ^{15}O-water are proportional to blood flow. Thus, the imaging time is ultimately limited by the point at which the signal is increasing slower than the image noise.

The aim of this study was to investigate how signal and

Received Feb. 28, 1994; revision accepted Jul. 26, 1994.

For correspondence and reprint requests contact: Simon R. Cherry, Imaging Sciences Division, Crump Institute for Biological Imaging, UCLA School of Medicine, 10833 Le Conte Ave., Los Angeles, CA 90024-6948.

noise change as a function of imaging time in PET activation studies using ^{15}O-water. Based on this information, we suggest a new paradigm based on switching between baseline and activation conditions (and vice-versa) in the middle of the study (switched protocol). This is an extension of an idea initially presented by Volkow et al. (*17*) and permits the difference signal between the two studies to be maintained for longer. This allows the imaging time to be extended leading to an improvement in S/N in the subtracted datasets. Temporal effects have also been studied by Hurtig et al. (*18*), who have demonstrated robust findings when the activation task is presented for only 20 sec, centered on the arrival time of the bolus in the brain. This is particularly useful when dealing with inattentive subjects or for studying short neuropsychologic events with PET.

In this paper, we address the switched protocol, both experimentally and with model simulations. Further issues include optimal imaging time, optimal switching time, sensitivity to switching time, sensitivity to bolus duration and the gain in S/N.

SIMULATIONS

The Model

A computer model was set up to simulate the idealized kinetics of ^{15}O-water in brain tissue. A standard two-compartment model representing ^{15}O-water in the plasma and tissue was assumed. The forward rate constant K_1 represents the product of blood flow per unit weight of tissue, F, and the single-pass extraction fraction E which can further be expressed in terms of the permeability-surface area product PS as (*19,20*):

$$K_1 = FE = F(1 - \exp^{-PS/F}). \quad \text{Eq. 1}$$

The value of PS for ^{15}O-water was assumed to be flow dependent as described by Herscovitch et al. (*12*):

$$PS = 1.50F + 0.21. \quad \text{Eq. 2}$$

For a passively diffusible tracer, K_1 and k_2 differ by the partition coefficient, which for these simulations is assumed to have a value of 1.00 ml/g (*21*). Using the conservation of mass, the exchange of tracer between the two compartments can then be written as:

$$\frac{dC_t(t)}{dt} = K_1C_a(t) - k_2C_t, \quad \text{Eq. 3}$$

where C_a and C_t are the concentrations of ^{15}O-water in blood and tissue, respectively. Solving this first order differential equation for the tissue concentration leads to:

$$C_t(T) = K_1\int_0^T C_a(t)\exp^{-k_2(T-t)}\,dt. \quad \text{Eq. 4}$$

The PET scanner sees the sum of the ^{15}O activity in the blood and the tissue compartments. The PET signal is also diminished as a function of time due to radioactive decay of ^{15}O. The relative signal detected by the PET scanner (assuming no deadtime losses), C_{PET}, can therefore be written as:

$$C_{PET}(T) = (V_tC_t(t) + V_aC_a(t))\exp^{-\lambda t}$$

$$= \left(V_tK_1\int_0^T C_a(t)\exp^{-k_2(T-t)}\,dt + V_aC_a(t)\right)\exp^{-\lambda t}, \quad \text{Eq. 5}$$

where λ is the decay constant for ^{15}O. Combining Equations 1 and 5 together, we obtain:

$$C_{PET}(T) = \left\{V_tF(1 - \exp^{-PS/F})\int_0^T C_a(t)\exp^{-k_2(T-t)}\,dt + V_aC_a(t)\right\}\exp^{-\lambda t}. \quad \text{Eq. 6}$$

By setting the fractional tissue and blood volumes to physiologically reasonable values of 0.95 ml/g and 0.05 ml/g (*22*) respectively, $C_{PET}(t)$ can be calculated for any given input function $C_a(t)$ and flow F. For these simulations, $C_a(t)$ was assumed to be of the form (*23*):

$$C_a(t) = \left(\frac{At}{p^2}\exp^{-t/P} + B\right)\exp^{-\lambda t}, \quad \text{Eq. 7}$$

where A and B are constants and P is the peak time. B represents recirculation of the tracer. The shape of this curve closely resembles that obtained in human studies following an intravenous bolus injection. The duration of the bolus can be altered by changing the value of P. The input function used for most of the following simulations (peak at 10 sec, A/B = 625) is shown in Figure 1.

This model makes the standard assumptions regarding tracer kinetic studies and compartmental models (*24*). Several variables, such as partition coefficient and fractional volumes of compartments have been fixed at physiologically sound values to simplify the presentation of the data. Further justification for this simplification is that the resulting time-activity curves are very insensitive to these parameters over any physiologically reasonable range of values.

Time-Activity Curves

The relationship between K_1 and k_2, assuming a partition coefficient of unity is:

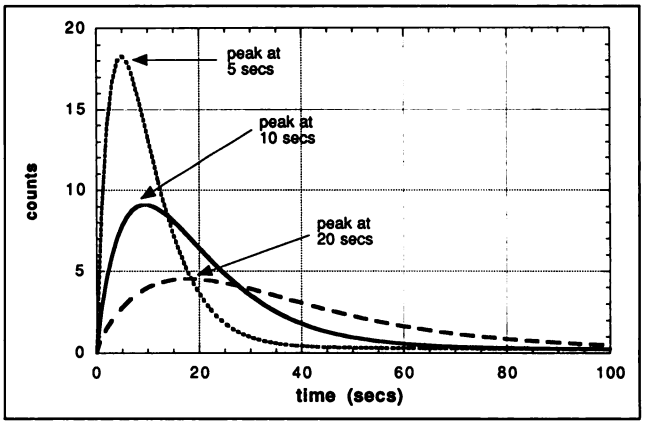

FIGURE 1. Input functions used in computer simulations that consist of two components describing the short bolus followed by tracer recirculation. Bolus duration is variable. The input function which peaks at 10 sec corresponds closely with dispersion corrected input functions obtained from direct radial artery sampling during rapid bolus ^{15}O-water injection in human subjects.

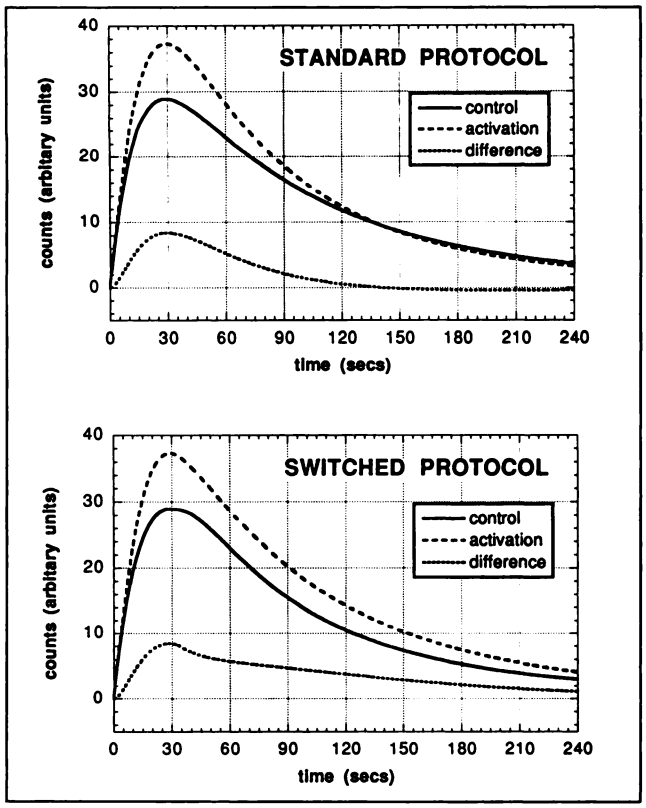

FIGURE 2. Top: Time-activity curves for a region of the brain during baseline (flow = 65 ml/min/100 g) and during activation (flow = 91 ml/min/100 g) using the standard protocol. The difference (activation-baseline) is also shown. Faster washout in the activation study ultimately leads to higher uptake in the baseline state relative to the activated state. Bottom: Time-activity curves under same conditions as above, except using the switched protocol. The difference signal (activation-baseline), is increased at later times relative to the standard protocol, by switching the task when the peak activity is reached.

$$K_1 = FE = k_2. \qquad \text{Eq. 8}$$

For a highly diffusible tracer such as ^{15}O-water, the extraction fraction $E \approx 1$ and so $K_1 \approx k_2 \approx F$. Thus, both the uptake of tracer and the subsequent rate of tracer washout are highly flow dependent. The autoradiographic method for measuring rCBF with PET makes use of the fact that the amount of tracer washout is small at early times, and therefore initial uptake is strongly dominated by blood flow. Thus, the PET data can be integrated for a short period following bolus arrival to yield a map of ^{15}O-water uptake which is closely proportional to rCBF.

Now consider what happens in an activation study, where the aim is to maximize the difference between scans acquired under two different sets of conditions. Simulated time-activity curves (from Eq. 6) for a region of gray matter at rest (F = 65 ml/min/100g) and after activation (F = 91 ml/min/100g, 40% activation) are shown in Figure 2 (top). The difference in blood flow initially leads to an increase in uptake of ^{15}O-water in the activated state relative to the control state as predicted by the autoradiographic method. At longer times, because of more rapid washout from the high-flow region the difference between control and activated states diminishes rapidly. In this case, after 140 sec or so there is actually higher uptake in the control study. This illustrates why

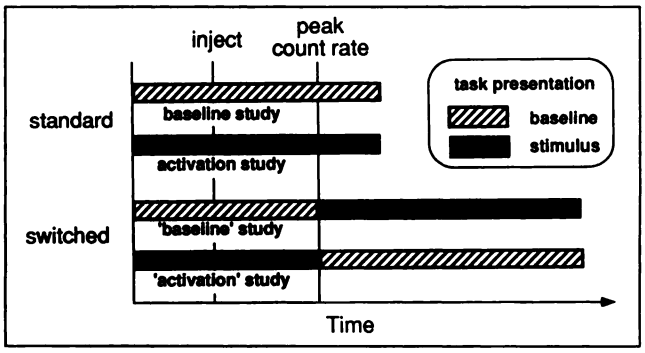

FIGURE 3. Schematic representation of time course of standard and switched protocols for activation studies.

the optimal integration length for PET rCBF activation studies using the autoradiographic method is around 60–90 sec. This optimal time will in practice be governed by a number of factors such as the injected dose, the sensitivity and deadtime characteristics of the scanner and the magnitude of resting and activated blood flows.

The Switched Protocol

To maintain the difference (activation minus control) signal over a longer period of time, thus permitting longer imaging times and improved S/N, we propose utilizing a different time sequence for the baseline and activation conditions. A previous study suggested, and showed some evidence in favor of, terminating the stimulus after the bolus of activity had been delivered (*17*). The rationale for this was that the high flow region in the activation study would quickly return to baseline flow values, thus reducing subsequent washout from the region. We take this concept a step further by also implementing the converse, applying the stimulus during the baseline study, after the bolus of activity is delivered, to increase washout from the activated region, in the baseline scan.

This we define as a switched protocol and is shown schematically in Figure 3. We have assumed the stimulus is switched on or off when peak activity is observed in the PET count rate (in this case at 30 sec). This is a point which is easy to monitor externally on most commercial PET systems. Functional MRI studies have demonstrated that the vascular response to a stimulus requires 3–5 sec (*2,4*) and so in the simulated data the switch from control to activated flows, or vice-versa, was implemented as a linear change over a 5-sec time period. The effect of the switched protocol on the time-activity curves is shown in Figure 2 (bottom) and demonstrates that the difference between activated and control scans is maintained over a longer period of time. This difference forms the signal in a PET activation subtraction study, and these simulations suggest that it may be possible to extend the imaging time and achieve significantly higher S/N using switched protocols.

Signal-to-Noise in Integrated Images

We are seeking to maximize S/N in the subtracted images. We can get a relative estimate of S/N from:

$$S/N = \frac{A - B}{\sqrt{A + B}}, \qquad \text{Eq. 9}$$

where A and B are the counts in the activation and baseline study from a particular part of the brain. If we plot the S/N as a function

of PET scan length for the simulated time-activity curves shown in Figure 2, we get the results shown in Figure 4. There are several features to notice: First, in the standard protocol, the S/N peaks for an integration time of approximately 70–80 sec after bolus arrival (taken to be t = 10 sec in Fig. 1) in the brain. This agrees with experimentally determined optimal scan lengths for the autoradiographic method *16*, and Grafton ST, *personal communication*. For longer integration times, the signal difference is increasing slower than the increase in noise due to improved statistics, hence the S/N ratio drops. In the switched protocol, the signal is maintained over a longer time period, therefore the peak S/N is higher and occurs for a longer integrated scan length. The simulations predict a 60% increase in peak S/N using switched protocols and a longer acquisition time relative to the standard protocol under these idealized conditions. Another interesting feature is that just after the switch is initiated, the switched protocol shows a small reduction in S/N relative to the standard protocol. This implies that the switch is being made too early and is more fully investigated below.

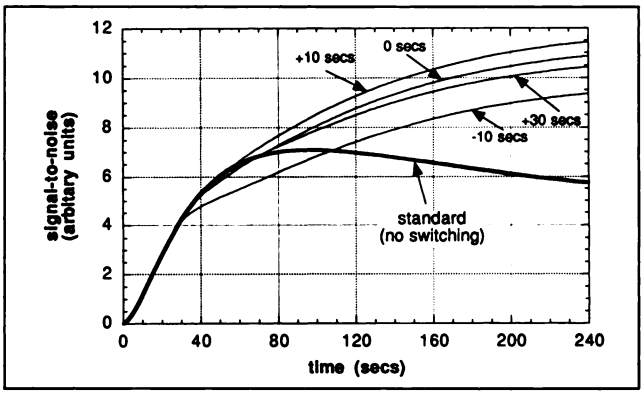

FIGURE 5. The effect of the switch time relative to the time of peak counts in the PET scanner (30 sec). The peak S/N value is relatively insensitive to switch times in the range 0–30 sec after the peak count rates is observed.

Effects Related to Switching Time

The time at which the switch between activating and baseline conditions is made is likely to be important. The optimal switching time will represent a balance between allowing enough time for the tracer to be delivered, and making the switch before significant washout has occurred. The effectiveness of the switched protocol will depend strongly on the combination of switching time which we investigate in this section, and the duration of the input bolus which is examined in the next section.

Using the input function which peaks at 10 sec, we performed simulations using a switch time of −10, 0, +10 and +30 sec relative to the peak count rate observed in the tissue curves which occurred at 30 sec (Fig. 2). Relative S/N values as a function of PET scan integration length were once again calculated using Equation 9 and are displayed for different switching times in Figure 5. These curves show that the peak S/N achieved is relatively insensitive to the time of the switch as long as the switch is not made too early. The simulations suggest that the time of peak count rate is too early and that the best S/N is obtained by making the switch some 10 sec after the peak count rate is recorded.

Although these results come from one specific simulation, the fact that there is a broad window of opportunity for making the switch and still effecting a significant improvement in S/N is encouraging. Since the timing of the switch is not too critical, the switched protocol should be relatively easy to implement, using the peak count rate as a guide to the earliest time that the switch between conditions should be made.

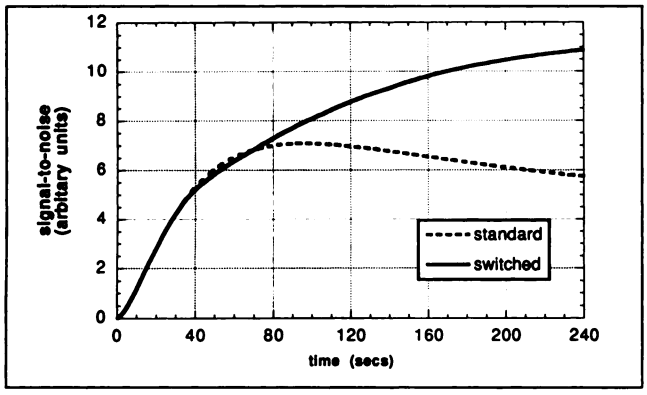

FIGURE 4. Signal-to-noise as a function of PET scan length for the standard and switched protocols. The standard protocol peaks at 90 sec; the switched protocol peaks much later and with a significant improvement in S/N.

Effects of Bolus Duration

One of the critical issues is the time course of tracer delivery. The switched protocol essentially tries to separate the study into the uptake and washout phases, therefore one might expect that the shorter the bolus duration, the better. To investigate this, we ran simulations for the same activation as presented previously (40% activation from 65 ml/min/100 g resting flow) and examined the effect of changing the bolus duration while still delivering the same total amount of activity. The bolus duration is quoted in terms of the time to peak parameter, P, for the input function as described by Equation 7 and the switching time is at the peak count rate. Figure 6 (top) shows that the standard protocol is relatively insensitive to bolus duration as one might expect. There is a small S/N advantage in using a shorter bolus, but the effect is less than 10%. The switched protocol, however, is much more sensitive to bolus duration (Fig. 6, bottom). The difference in S/N between using a fast bolus (5 sec to peak) and slow bolus (20 sec to peak) is 50%. With a slow bolus, the resultant S/N is not much better than that obtained using the standard protocols, because the distinction between the uptake phase and the washout phase becomes blurred. Recirculation of tracer will also play a role in determining the effectiveness of the switched protocol, because this leads to tracer delivery during the washout phase. A realistic amount of recirculation was modeled in these simulations (Fig. 1) although a systematic study was not carried out since the amount of recirculating tracer is not under the control of the investigator.

Effects of Activation Magnitude

In this simulation, the magnitude of the activation was varied between 5% and 50% to see if the S/N gains predicted for the switched protocol show any dependency on the magnitude of the activation. Figure 7 shows the ratio between the peak S/N for the standard and switched protocols as a function of activation magnitude. The simulation shows that the S/N gain is very insensitive to activation magnitude, and that the switched protocol gives gains of 60% in S/N over the entire range of interest.

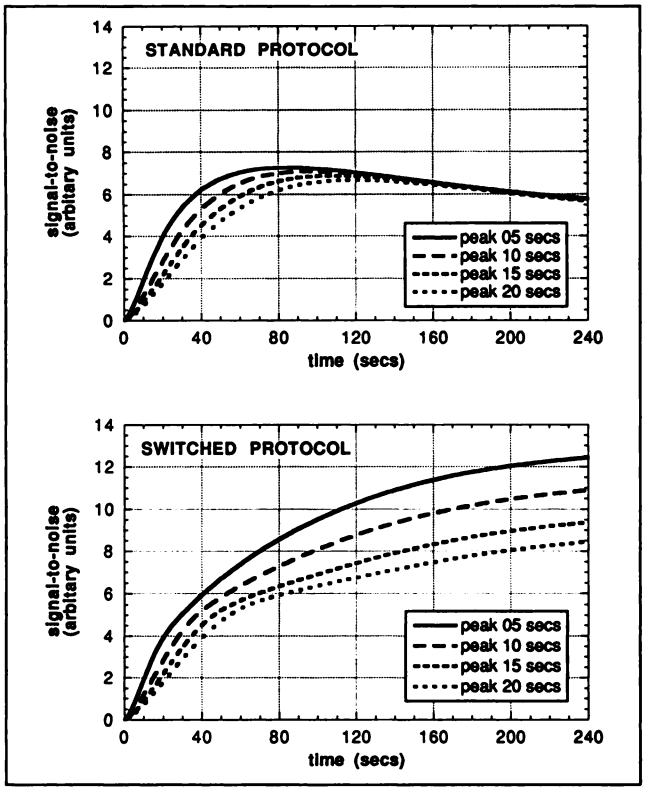

FIGURE 6. Top: S/N as a function of input function duration for the standard protocol (top) and the switched protocol (bottom). The S/N versus integration time is relatively insensitive to bolus shape with the standard protocol. In contrast, the switched protocol relies on a short bolus to separate the data into "uptake" and "washout" phases, therefore bolus duration is a critical determinant of S/N.

Simulation Summary

The simulations predict that significant gains in S/N can be realized by employing a switched protocol which attempts to split the data acquisition into uptake and washout phases. It appears that the optimum time for making the switch is just after the peak count-rate is recorded in the scanner. The timing of the switch is not critical in determining the S/N gain as long as the switch is made within 30 sec following the time of peak count rate. This 30-sec window represents the time in which uptake and washout of tracer are approximately balanced and can be regarded as a static period between the uptake and washout phases of the acquisition. The bolus duration should be as short as possible to help separate uptake and washout phases cleanly. The S/N gain realized with the switched protocols relative to the standard protocol is predicted to be virtually independent of activation magnitude.

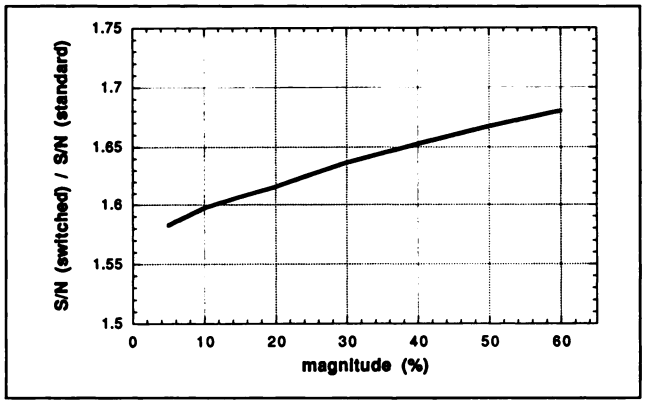

FIGURE 7. Signal-to-noise as a function of activation magnitude for the switched protocol relative to the standard protocol. Large S/N gains are predicted independent of the activation magnitude.

MATERIALS AND METHODS

Human Studies

Studies were performed in five normal volunteers who gave informed consent under the guidelines issued by the UCLA Human Subject Protection Committee. Eight PET studies were performed in each of the subjects, using an injected dose of 10 mCi of ^{15}O-water. PET scans were obtained using the ECAT-831 brain PET system in the three-dimensional mode (*5,7*) and the data reconstructed using a fully three-dimensional reconstruction algorithm (*25,26*).

In the first four subjects, the stimulus consisted of a full-field reversing (7.8 Hz) checkerboard pattern, which has been previously shown to lead to strong activation in the primary visual cortex (*27*). The baseline condition consisted of a stationary gray display. In each subject, the following studies were performed: 2 × continuous baseline, 2 × continuous activation, 2 × switched baseline and 2 × switched activation. In the switched studies, conditions were reversed when the peak count-rate was observed from the scanner. In all cases, task conditions were established 20 sec prior to injection of the ^{15}O-water and the bolus (volume approximately 7 cc) was injected over 5 sec. PET data was acquired dynamically as six frames (25 sec, 30 sec, 35 sec, 40 sec, 50 sec and 60 sec) starting from the time activity was registered by the scanner. Integrated scans were created from the dynamic sequence corresponding to 25-, 55-, 90-, 130-, 180- and 240-sec acquisitions following activity arrival in the brain. Baseline studies were subtracted from activation studies after global normalization to produce difference maps for each of these scan lengths. Regions of interest (ROIs) were drawn over the visual cortex (signal) and over other nonactivated gray matter regions (noise) to determine S/N for both standard and switched protocols. The ROIs were defined for each subject individually using the sum of all time points from both the switched and standard data. This prevents any bias towards one protocol or the other and keeps the ROI constant for all different time points within an individual. The regions were then copied to the individual frames of each dataset and ROI values determined for each of the four conditions as a function of time.

In the fifth subject, we utilized a motor tracking task that has been used extensively in our laboratory. This task was described in detail by Grafton et al. (*28*) and requires the subject to track a 0.5-cm target moving at 6 cm/sec and changing direction 200 times/min in a 6 × 8-cm field. This task produces activation of the contralateral primary motor cortex as well as the premotor and supplementary motor areas. The subject was instructed to point to the object continuously with the right index finger (utilizing movements of the wrist and elbow) during the activation components of the tasks and to follow the target with his eyes only during the control components. During switched protocols, the subject was prompted to change tasks at the appropriate time by having the investigator say the word "switch". Signal-to-noise estimates were determined by ROI analysis as described above, using the primary motor cortex and premotor activation sites for the signal,

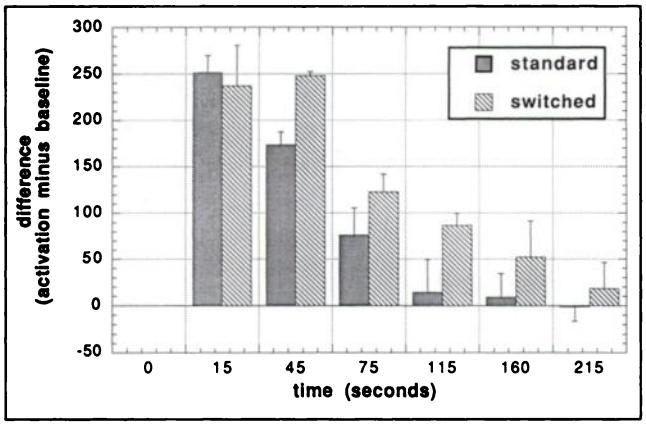

FIGURE 8. Signal (activation minus control) as a function of time for standard and switched protocols. Average of four subjects. Note retention of signal in switched protocols relative to standard protocol as time progresses. Signal in the first frame is collected before the switch occurs and thus shows no significant difference between protocols.

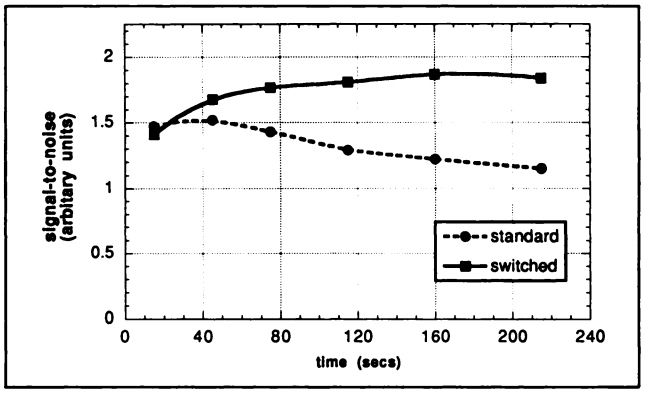

FIGURE 10. Signal-to-noise as a function of PET scan length for both protocols. Curves show same general trends as the simulations in Figure 6, although the S/N gain from using the switched protocols is somewhat lower than predicted.

and similar sized ROIs over nonactivated gray matter areas to determine the noise.

RESULTS

Figure 8 shows the difference signal (activation minus control) for both the standard and switched protocols as a function of time in the visual cortex, averaged across all four subjects. The subtraction images from one subject are shown in Figure 9. Both these figures clearly show that the signal is maintained for a longer time period by using the switched protocol as predicted by the simulations. The peak count rate was observed at approximately 25 sec after the arrival of activity in the brain and was very consistent from trial to trial. The signal from the first frame (0–25 sec), which is collected before the switch is made, is identical for both protocols as expected. The S/N estimates as a function of integrated PET scan duration, determined from ROI analysis, are shown in Figure 10 for both protocols. Again, there is concordance between the simulated and experimental datasets (compare with Fig. 4), with a peak at around 70 sec for the standard protocol and a plateau established at longer times for the switched protocol. The peak S/N gain is approximately 25%. This is less than predicted by the simulations, but is a substantial gain nonetheless.

In the motor-tracking task, which produces a smaller activation magnitude compared with the visual task, the switched protocol resulted in a 20% improvement in S/N. This shows that the improvement is not a strong function of the activation magnitude as predicted by the simulations.

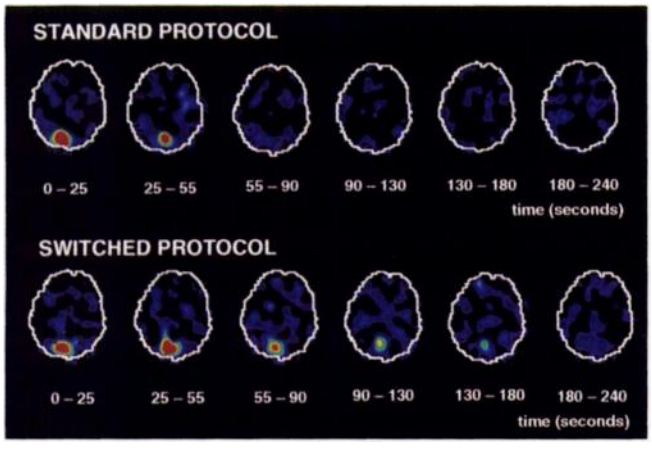

FIGURE 9. Signal (activation minus control) as a function of time for standard and switched protocols in one of the four subjects. Notice retention of difference signal in visual cortex in the switched protocol out to 180 sec.

DISCUSSION

We have demonstrated the ability to improve S/N in PET activation studies by using switched protocols which take advantage of the uptake and washout kinetics of ^{15}O-water. These methods could be applied equally well to centers which use ^{15}O-butanol as a blood flow tracer. The increase in S/N seen in the experimental studies averaged 25% compared with 60% predicted by the simulations. The discrepancy is probably attributable to a number of factors. First, PET scanner deadtime will result in counts being preferentially lost during the early phase of the study. This results in a smaller signal gain than predicted by the simulations and thus, a reduction in the S/N gain. Another major issue is the validity of the simple two-compartment model for rapidly exchanging tracers. It has been previously shown that this model is inadequate to describe all the features of the kinetics of highly diffusible tracers (*29*) and so it is not surprising that it predicts the correct trends but not the correct magnitudes. A 25% gain in true S/N is still a very significant improvement and would allow equivalent statistics to be obtained using two-thirds of the injected dose or number of subjects. This is of particular value since it would further decrease the administered dose to normal volunteers. Combining three-dimensional data acquisition, dose fractionation and switched protocols al-

lows high quality activation datasets to be obtained using less than 10 mCi per trial and less than 150 mCi in total.

Switched protocols are particularly well suited to experiments in which the primary sensory input is the only variable that changes between activation and control; in such cases, the switch is completely under control of the investigator and does not require any cooperation or effort on the part of the subject. However, the motor task that we used demonstrates that it is possible to use switched protocols to improve S/N in situations where the two tasks differ only in terms of the instructions that the subject must follow. While new cognitive dimensions are added to the tasks by requiring the subjects to listen for and hear the word "switch" and to remember the nature of the task to be performed after the switch, these dimensions are similar in the activation-control and control-activation tasks minimizing their impact on the subtracted images. Furthermore, since wash-in and wash-out are near equilibrium at the time of the switch, any differences in switching from activation to control as compared to switching from control to activation (e.g., lowering the arm in one case and raising it towards the screen in the other) are predicted to have minimal impact. Nonetheless, the possibility that these additional cognitive requirements may interact with the primary tasks must be carefully considered in designing and interpreting switched protocol experiments. In some situations (e.g., two different stimuli versus baseline conditions) it may be desirable to use "semi-switched" protocols where the stimulus is removed during the activation study, but not applied in the baseline study. This leads to roughly half the gain shown for the fully switched protocols.

A very important point is that the use of the switched protocol does not preclude quantitative assessment of rCBF using the autoradiographic technique. According to the simulations, S/N is maximized if the switching point occurs between 50 and 80 sec postinjection. This is longer than the optimal integration time determined for quantitative rCBF imaging using the autoradiographic technique (*12,14*). Thus, the study can be acquired in two frames, using a short duration frame of 40 sec for quantitative assessment of rCBF, and the sum of this frame with a second frame encompassing the period determined to give the maximum S/N with the switched protocol. Since the switch occurs after completion of the first frame, it will not affect the quantitative data. Employing this type of protocol leads to data which can be expressed quantitatively or in a manner which maximizes S/N.

The switched paradigms are an attempt to exploit the known kinetics of rapidly diffusible tracers to maximize this difference. The whole concept of manipulating tracer kinetics to maximize differences between states or conditions is potentially a powerful tool which might also be useful in other PET applications. We intend to explore this concept further, and use simulations and experimental data to further refine the optimal activation protocol for ^{15}O-water studies.

ACKNOWLEDGMENTS

The authors thank the staff of the cyclotron and PET center at UCLA for their technical support of this work and Lars Eriksson for useful discussions. This work was supported by Department of Energy Contract DE-FC03-87ER 60615, NIMH Grant R01-MH37916, NIH-NINDS grant P01-NS15654 and NCI grant R01-CA56655.

REFERENCES

1. Mazziotta JC, Phelps ME. Positron emission tomography studies of the brain. In: Phelps M, Mazziotta J, Schelbert H, eds. *Positron emission tomography and autoradiography.* New York: Raven Press, 1986:493–579.
2. Ogawa S, Tank DW, Menon R, et al. Intrinsic signal changes accompanying sensory stimulation: function brain mapping with magnetic resonance imaging. *Proc Natl Acad Sci* 1992;89:5951–5955.
3. Kwong KK, Belliveau JW, Chesler DA, et al. Dynamic magnetic resonance imaging of human brain activity during primary sensory stimulation. *Proc Natl Acad Sci* 1992;89:5675–5679.
4. Bandettini P, Wong E, Hinks R, Tikofsky RS, Hyde JS. Time course EPI of human brain function during task activation. *Mag Res Med* 1992;25:390–397.
5. Cherry SR, Dahlbom M, Hoffman EJ. Three-dimensional PET using a conventional multislice tomograph without septa. *J Nucl Med* 1991;15:655–668.
6. Townsend DW, Geissbuhler A, Defrise M, et al. Fully three-dimensional reconstruction for a PET camera with retractable septa. *IEEE Trans Med Imag* 1991;10:505–512.
7. Cherry SR, Woods RP, Hoffman EJ, Mazziotta JC. Improved detection of focal cerebral blood flow changes using three-dimensional positron emission tomography. *J Cerebr Blood Flow Metab* 1993;13:630–638.
8. Woods RP, Cherry SR, Mazziotta JC. Rapid automated algorithm for aligning and reslicing PET images. *J Comput Assist Tomogr* 1992;16:620–633.
9. Woods RP, Mazziotta JC, Cherry SR. MRI-PET registration with automated algorithm. *J Comput Assist Tomogr* 1993;17:536–546.
10. Worsley KJ, Evans AC, Marrett S, Neelin P. A three-dimensional statistical analysis for CBF activation studies in human brain. *J Cereb Blood Flow Metab* 1992;12:900–918.
11. Friston KJ, Frith CD, Liddle PF, Frackowiak RSJ. Comparing functional (PET) images: the assessment of significant change. *J Cereb Blood Flow Metab* 1991;11:690–699.
12. Herscovitch P, Markham J, Raichle ME. Brain blood flow measured with intravenous $H_2{}^{15}O$. I. Theory and error analysis. *J Nucl Med* 1983;24:782–789.
13. Mazziotta J, Huang S-C, Phelps ME, Carson RE, MacDonald NS, Mahoney K. A noninvasive positron computed tomography technique using oxygen-15-labeled water for the evaluation of neurobehavioral task batteries. *J Cereb Blood Flow Metab* 1985;5:70–78.
14. Raichle ME, Martin WRW, Herscovitch P, Mintun MA, Markham J. Brain blood flow measured with intravenous $H_2{}^{15}O$. II. Implementation and validation. *J Nucl Med* 1983;24:790–798.
15. Kanno I, Iida H, Miura S, Murakami M. Optimal scan time of oxygen-15-labeled water injection method for measurement of cerebral blood flow. *J Nucl Med* 1991;32:1931–1934.
16. Mintun MA, Raichle ME, Quarles RP. Length of PET data acquisition inversely affects ability to detect focal areas of brain activation. *J Cereb Blood Flow Metab* 1989;9 (Suppl 1):S349.
17. Volkow ND, Mullani NA, Gould LK, Adler SS, Gatley SJ. Sensitivity of measurements of regional brain activation with oxygen-15-water and PET to time of stimulation and period of image reconstruction. *J Nucl Med* 1991; 32:58–61.
18. Hurtig RR, Hichwa RD, O'Leary DS, et al. Effects of timing and duration of cognitive activation in [^{15}O]water PET studies. *J Cereb Blood Flow Metab* 1994;14:423–430.
19. Crone C. The permeability of capillaries in various organs as determined by the use of the "indicator diffusion" method. *Acta Physiol Scand* 1963;58: 292–305.
20. Renkin EM. Transport of potassium-42 from blood to tissue in isolated mammalian skeletal muscles. *Am J Physiol* 1959;197:1205–1210.
21. Eichling JO, Raichle ME, Grubb RL, et al. Evidence of the limitations of water as a freely diffusible tracer in brain of Rhesus monkey. *Circ Res* 1974;35:358–364.
22. Phelps ME, Mazziotta JC, Huang S-C. Study of cerebral function with

positron computed tomography. *J Cereb Blood Flow Metab* 1982;2:113–162.
23. Iida H, Kanno I, Miura S, Murakami M, Takahashi K, Uemura K. Error analysis of a quantitative cerebral blood flow measurement using $H_2{}^{15}O$ autoradiography and positron emission tomography with respect to the dispersion of the input function. *J Cereb Blood Flow Metab* 1986;6:536–545.
24. Huang S-C, Phelps ME. Principles of tracer kinetic modeling in positron emission tomography and autoradiography. In: Phelps M, Mazziotta J, Schelbert H, eds. *Positron emission tomography and autoradiography.* New York: Raven Press, 1986:287–346.
25. Defrise M, Townsend DW, Geissbuhler A. Implementation of three-dimensional image reconstruction for multi-ring tomographs. *Phys Med Biol* 1990; 35:1361–1372.
26. Cherry SR, Dahlbom M, Hoffman EJ. Evaluation of a 3D reconstruction algorithm for multi-slice PET scanners. *Phys Med Biol* 1992;37:779–790.
27. Fox PT, Raichle ME. Stimulus rate determines regional blood flow in striate cortex. *Ann Neurol* 1985;17:303–305.
28. Grafton ST, Woods RP, Mazziotta JC, Phelps ME. Somatotopic mapping of the primary motor cortex in humans: activation studies with cerebral blood flow and positron emission tomography. *J Neurophysiol* 1991;66:735–743.
29. Larson KB, Markham J, Raichle ME. Tracer-kinetic models for measuring cerebral blood flow using externally detected radiotracers. *J Cereb Blood Flow Metab* 1987;7:443–463.